Gait Generation of Hexapod Robot for the CPG Controller by Using the Delayed Van der Pol Oscillators

Zigen Song（✉ zgsong@tongji.edu.cn ）

Tongji University

Jiayi Zhu

Shanghai Ocean University

Jian Xu

Tongji University

Gait Generation of Hexapod Robot for the CPG Controller by Using the Delayed Van der Pol Oscillators

Zigen Song[1]

E-mail: zgsong@tongji.edu.cn,

School of Aerospace Engineering and Applied Mechanics, Tongji University, Shanghai, 200092, China

Jiayi Zhu

E-mail: m200711430@st.shou.edu.cn,

College of Information Technology, Shanghai Ocean University, Shanghai 201306, China

Jian Xu

E-mail: xujian@tongji.edu.cn,

School of Aerospace Engineering and Applied Mechanics, Tongji University, Shanghai, 200092, China

Abstract：In this study, we construct a type of CPG (central pattern generator) controller by using the delay-coupling Van der Pol (VDP) oscillators and propose an analysis method of parameter modulation to illustrate the locomotion gait of a hexapod robot. The structure topology of the CPG controller is scheduled as a unidirectional ring network consisting of six identical units. Each unit has independent parameters to modulate amplitude and frequency of the period activity. Employing the Hopf bifurcation, we first propose parameter conditions to guarantee the existence of the period activity for the delayed CPG controller, where coupling delay can induce generation and extinction of the period activity. Due to the symmetry structure of the proposed CPG controller, the period activity induced by coupling delay presents multiple spatiotemporal patterns with a constant phase difference. Based on theoretical analysis of the equivariant Hopf bifurcation, we further pinpoint parameter regions for the corresponding spatiotemporal patterns. Then using the invariable phase difference between signal outputs of the VDP oscillators, we assign connection order of the CPG units to link the hexapod's legs and produce the hexapodal locomotion gaits. The results show that the coupling delay in the delayed VDP-CPG controller is an effective method to obtain many types of the hexapodal locomotion gaits.

Keywords: CPG (Central pattern generator); delay coupling; VDP oscillator; hexapod locomotion gait; dynamical analysis method.

[1] Corresponding author.

1. Introduction

Biological researches have shown that gait locomotion of animals, including vertebrates and invertebrates, is initiated and controlled by a special neural network called as the central pattern generator (CPG) system, which produces rhythm patterns to alternate coordination of the flexor and extensor motor-neurons (Grillner and Manira, 2019; Wang et al., 2021; Lobato-Rios et al., 2022). From an application perspective of bio-robotic engineering, the CPG neural network is regarded as a distributed system composed of nonlinear coupling oscillators. Phase relationship of the rhythmic controlling signals are produced to present different gait patterns. Many types of artificial CPG neural systems are proposed to obtain stable and smooth gait locomotion (Yu et al., 2014; Kinugasa and Sugimoto, 2017; Ryczko et al., 2020).
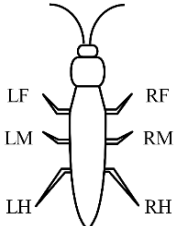
In fact, the bio-inspired CPG controlling strategies have great advantage to steer robots with multiple degrees of freedom (DOF). It can coordinate movement of all joints by adjusting a few parameters and avoid reluctant modeling process of the model-based control method (Holmes et al., 2006). Inspired by the swimming CPG of lamprey, Ijspeert and his cooperators (Ijspeert 2001; Ijspeert et al., 2007) constructed CPG controllers based on the coupled ACPO model (amplitude controlled phase oscillator) to steer swimming and crawling of the biomimetic robots, such as salamander robot, fish robot, and snake robot. For legged robots, quadruped locomotion have been extensively investigated by many researchers from theoretical analyses and experimental researches (In et al., 2022). Hexapod walking robot is inspired by insect's locomotion (Inagaki et al., 2003; 2006; Goldman et al., 2006). Chen et al. (2012) constructed a hexapod robot and obtained smooth transition of gait locomotion by using a CPG controller with isochronous oscillator and first-order low-pass filter. Feedback information of the vision was integrated to adjust movement speed of a hexapod robot and obtain smooth transition of gaits within a simplified experimental environment (HugoBarron-Zambrano et al., 2015). Using VDP oscillators with a diffusive coupling scheme, Yu et al., (2016) proposed a hexapod CPG-based controlling method to obtain wave, tetrapod and tripod gait patterns and their smooth transitions. The CPG neural network combined with a feed-forward self-adaptive control method was proposed to realize a crab-like robot walking on complex terrain (Wang et al., 2017). Chang and Mei (2018) designed a controlling strategy consists of central neural system (CNS) and CPG to realize an ant-like gait and its transition. Employing the Hopf oscillator with bidirectional diffusive coupling, Bal (2021) obtained a smooth transition of the biomimetic hexapoda gaits. Recently, the reinforcement learning strategy was employed to adjust controlling parameters of the hexapod CPG controller based on the Hopf oscillators (Ouyang et al., 2021) and spiking neural networks (Lele et al., 2020).

To obtain flexible locomotion under unstructured environment for the bio-inspired robots, the proposed CPG controllers should have many types of locomotion gaits to satisfy movement speed by switching the control parameters. Golubitsky and his coworkers (Golubitsky et al., 1998; 1999; Golubitsky and Stewart, 2016) presented a theoretical method to describe patterns relationship of locomotion gait by using the symmetric group theory. They further proposed the CPG controllers

composed of several nonlinear oscillators to obtain gait patterns of the bipedal locomotion (Pinto and Golubitsky, 2006; Stewart 2014) and quadruped locomotion (Buono and Golubitsky, 2001; Buono 2001; Stewart, 2017). For hexapodal locomotion, Collins and Stewart (1993) investigated model-independent features of the six-unit symmetrical networks and indicated that the hexapodal gait patterns and their switching can be obtained by using the standard symmetry-breaking bifurcation. Holmes and his coworkers adapted the six-interconnected three-dimensional bursting neurons to construct an insect cockroach CPG model and obtained the gait patterns for the high and low movement speed, i.e. tetrapod gait at low speed, tripod gait at high speed, and a unique branch of transition gaits (Ghigliazza and Holmes, 2004; Aminzare et al., 2018; Aminzare and Holmes, 2019). Further, Barrio et al. (2020) presented in detail the translating evolution of the dominant patterns by using numerical methods, i.e. the lateral phase lag analysis and quasi-Monte Carlo pattern sweeping.

The typical gait patterns of the hexapod walking robot are illustrated in Table 1, where we classify the locomotion gaits based on their phase relations of legs (L-left, R-right, F-front, M-middle, and H-hind). The LH-leg is selected as a reference position that is the phase difference is always at 0. For these hexapod locomotion gaits, there are four types of the normalized phase differences, i.e. 1/6, 1/4, 1/3, and 1/2. The sequence order of the leg's movement is to determine the type of the gait patterns. The pronk gait has a zero-phase difference between each other. All legs leave the ground simultaneously. For the classification of 1/6-phase difference, there are three types of locomotion patterns, i.e. wave (Kitsunai et al., 2020), metachronal (Inagaki et al., 2006; Collins and Stewart, 1993), and rolling tripod gaits (Inagaki et al., 2006; Golubitsky et al., 1998). Specifically, the wave gait has the sequence order of the leg's movement, i.e. {LF, RF, LM, RM, LH, RH}. The metachronal and rolling tripod gaits present their orders {LF, RH, LH, RM, LM, RF} and {LF, RH, LM, RF, LH, RM}, respectively. Similar results for the other gait patterns are shown in Table 1.

Table 1: The typical gait patterns of the hexapodal locomotion

Hexapod Robot	Phase Difference	Locomotion Gait Patterns	Sequence Order of Leg Movement (LF, LM, LH, RF, RM, RH)
	0	Pronk (Golubitsky et al., 1998)	0, 0, 0, 0, 0, 0
	1/6	Wave (Kitsunai et al., 2020)	0, 2/6, 4/6, 1/6, 3/6, 5/6
		Metachronal tripod (Inagaki et al., 2003; 2006; Collins and Stewart, 1993)	0, 5/6, 4/6, 3/6, 2/6, 1/6
LF RF		Rolling tripod (Inagaki et al., 2006; Golubitsky et al., 1998)	0, 2/6, 4/6, 3/6, 5/6, 1/6
LM RM	1/4	Tetrapod (Collins and Stewart, 1993)	0, 3/4, 1/2, 1/2, 1/4, 0
		Bowtie (Kitsunai et al., 2020)	0, 1/2, 1/2, 1/4, 3/4, 3/4
LH RH	1/3	Caterpillar gait (Golubitsky et al., 1998)	0, 2/3, 1/3, 0, 2/3, 1/3
		Rice (Kitsunai et al., 2020)	0, 2/3, 1/3, 1/3, 2/3, 0
	1/2	Tripod (Kitsunai et al., 2020; Collins and Stewart, 1993)	0, 1/2, 0, 1/2, 0, 1/2
		Pace (Golubitsky et al., 1998)	0, 0, 0, 1/2, 1/2, 1/2

In this study, based on the delay-coupling VDP oscillators with unidirectional ring structure, we propose a delayed VDP-CPG controlling strategy to obtain the above-mentioned locomotion gaits of the hexapod robot by employing a theoretical method of the dynamical analysis, which is our motivation of this paper. In fact, time delay of coupling oscillators is a very important factor to generate periodic activity and adjust their dynamical properties (Song et al., 2015; 2020; Yao et al., 2019). Based on the equivariant bifurcation theory of the delay differential equation, some authors investigated spatiotemporal patterns of the periodic activity (Atay and Ruan, 2015; Wang and Campbell, 2017). Time delay was once considered as a disadvantageous factor to avoid its destructive effect in the CPG network systems (Ohgane et al., 2009; Verdaasdonk et al., 2007; Lu et al., 2022). Based on the synchronization theory, Zhu et al. (2018; 2019) constructed locomotion gaits of the multi-legged robot by employing the coupling delay to adjust phase shift of the periodic activities. Recently, to apply regulating advantages of time delay on the spatiotemporal patterns, the delayed half-center oscillator (HCO) of the CPG system was proposed (Song and Xu, 2022) and realized the locomotion gaits of a snake-like robot (Song et al., 2022) and quadruped robot.

Notably, the presented theoretical method in this study has some advantages to construct the CPG controller. Firstly, the delayed VDP-CPG controller proposes few parameters to steer the hexapodal gaits. Adjusting time delay can obtain the above-mentioned locomotion gaits. Secondly, the delayed VDP-CPG controller proposes many types of locomotion gaits of the hexapod robot. Almost all of the gait patterns of hexapod locomotion can be obtained as in Table 1. Thirdly, the delayed CPG controller proposes an analytical strategy to obtain parameter regions of the gait patterns, which avoids too much trial-and-errors to choose the parameter values. Lastly, the different locomotion gaits can be switched rapidly without any intermediate states by adjusting time delay. This paper is organized as follows. In Section 2, we exhibit the dynamical analysis of the VDP oscillator and propose a topological structure of the CPG controller, i.e. unidirectional ring network consisting of six identical VDP oscillators. In section 3, employing the Hopf bifurcation analysis, we present the parameter conditions to guarantee the existence of the periodic activity in the delayed VDP-CPG controller. The periodic activity appears and disappears with increasing time delay. In section 4, we further give the spatiotemporal patterns of the periodic activity induced by time delay and illustrate the corresponding parameter regions by using theoretical analysis of the equivariant Hopf bifurcation. In section 5, we design the connection order of the CPG units to link the hexapod legs and produce locomotion gaits for the regions of the system parameters. Finally, in section 6, we give some conclusions.

2. The CPG model

The important and characteristic feature of CPG model is that the constructed network system can generate the stable periodic activity and appropriate spatiotemporal patterns in order to provide a rapid and smooth transition of locomotion gaits. The VDP oscillator is a simple and self-excited

nonlinear model, which has been applied in theoretical analyses and engineering applications. The VDP oscillator is governed by the following differential equation.

$$\ddot{x}(t) + \varepsilon \left(x^2(t) - \alpha \right) \dot{x}(t) + \beta x(t) = 0, \tag{1}$$

where $\alpha > 0$ and $\beta > 0$ determine the amplitude and frequency of the periodic activity, $\varepsilon > 0$ controls the periodic shape. The phase portraits of the VDP oscillator for the chosen parameters are show in Fig. 1(a) and (b). It follows that the increasing of α enhances the amplitude of the periodic activity. The shape of the periodic activity evolves from a sinusoidal-like wave into a relaxation oscillation as the parameter ε increases. Further, we exhibit the amplitude and frequency with the increasing of the parameters α and β, as shown in Fig. 1(c) and (d). The system parameters of the VDP oscillator can determine independently the amplitude and frequency of the periodic activity.

(a)

(b)

(c)

(d)
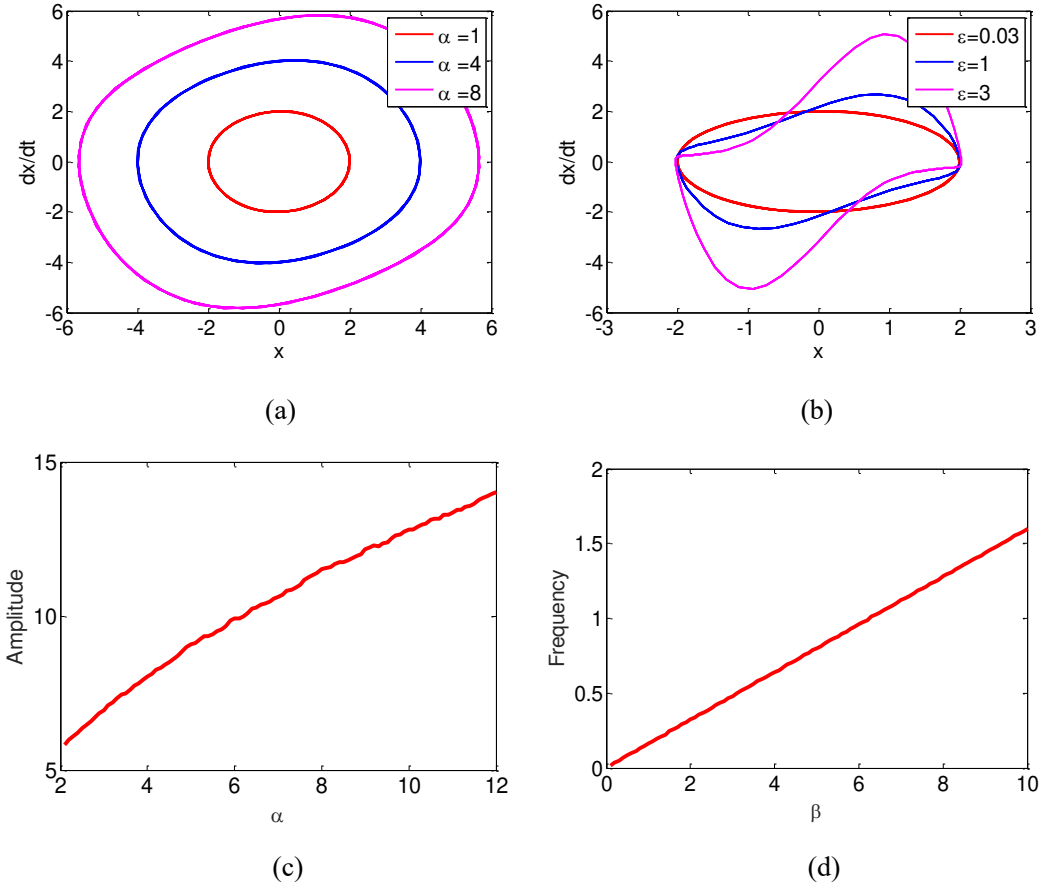
Fig. 1.   Phase portrait of the VDP oscillator exhibits the increasing of the amplitude and frequency with increasing parameters (a) increasing α for $\beta = 1$, $\varepsilon = 0.03$, (b) increasing β for $\alpha = 1$, $\varepsilon = 0.03$, (c) α-amplitude for $\varepsilon = 0.03$ and $\beta = 1$, and (d) β-frequency for $\varepsilon = 0.03$ and $\alpha = 1$.

Coupling connection between the oscillators in the CPG controller provides the generation of the spatiotemporal patterns and determines the output relationship of the periodic signals. An eminent topological connection can eliminate the number of controlling parameters and obtain more

robust activities to steer the robot locomotion under a variable and complicated environment. In our previous researches (Song and Xu, 2022; Song et al., 2022), delay coupling was introduced to construct the CPG controller. As matter of fact, the delayed CPG neural system easily proposes the periodic activity with multiple types of spatiotemporal patterns by employing the equivariant Hopf bifurcation. The dynamics of the CPG controller with coupling delay is presented as the following differential equation.

$$\ddot{x}_i(t) + \varepsilon_i \left(x_i^2(t) - \alpha_i \right) \cdot \dot{x}_i(t) + \beta_i x_i(t)$$
$$= k_i H\left(\dot{x}_i(t) \right) + \sum_{j=1, j \neq i}^{n} k_{ij} H\left(\dot{x}_j(t - \tau_{ij}) \right), \qquad i(\bmod n) \tag{2}$$

where k_i and k_{ij} are self- and mutual-coupling weights, τ_{ij} is time delay of coupling connection from the j-th oscillator to i-th, $H(x)$ is a neural activation function.
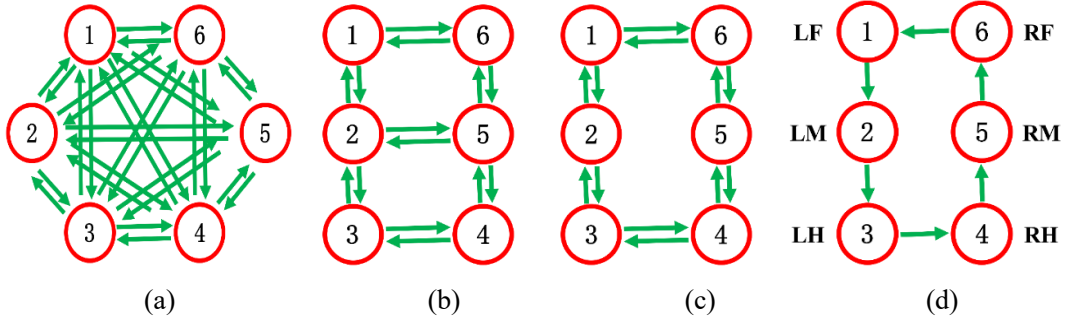
Fig. 2. Some network structures with six VDP oscillators: (a) fully connected network, (b) ladder-type network, (c) bidirectional ring network, and (d) unidirectional ring network.

To further determine topological structure of the CPG controller, we select some special network consisting of six VDP oscillators, as shown in Fig. 2. Fig. 2(a) is a fully connected network. Fig. 2(b) is a ladder-type network. Fig. 2(c) and (d) are the bidirectional and unidirectional ring networks. We have checked these types of network system. All CPG controllers can propose periodic activity for the applicable values of system parameters. However, the fully connected network has the more complex dynamical behaviors. The ladder-type network presents a periodic activity with different amplitude, which will induce more controlling parameters. The bidirectional ring network just exhibits two different patterns, i.e. synchronous and anti-synchronous periodic activities. The unidirectional ring network illustrated in Fig. 2(d) has a topological structure with Z_6 symmetry, which will induce the special spatiotemporal patterns to present different locomotion gaits of the hexapod robot. In this study, the proposed VDP-CPG controller with coupling delay is determined by the following delay differential equation, i.e.

$$\ddot{x}_i(t) + \varepsilon \left(x_i^2(t) - \alpha \right) \dot{x}_i(t) + \beta x_i(t) = -k \dot{x}_i(t) + k \dot{x}_{i+5}(t - \tau), \qquad i \bmod(6), \tag{3}$$

where all VDP oscillators are fixed as the same parameters. The self-coupling is selected as an

inhibition and inter-connection is excitation, which is $k > 0$ in system (3). We fix the activation function as the linear function $H(u) = u$. In the following section, we will analyze the periodic activity induced by the coupling delay and present rhythmic generation for the delayed VDP-CPG controller, which can be used to construct multiple types of locomotion gaits for the hexapod robot.

3. Rhythm generation of the CPG controller

To generate rhythm activity of the VDP-CPG controller with coupling delay, we consider the Hopf bifurcation of the trivial equilibrium. Obviously, system (3) proposes the trivial equilibrium $(0, 0, 0, 0, 0, 0, 0, 0, 0, 0, 0, 0)$. Employing $x_i \to x_i$, $\dot{x}_i \to y_i$, we can rewrite system (3) into the following first-order differential equation, which is

$$\begin{cases} \dot{x}_i(t) = y_i(t), \\ \dot{y}_i(t) = -\varepsilon \left(x_i^2(t) - \alpha \right) \cdot y_i(t) - \beta x_i(t) + k \left(y_{i+5}(t-\tau) - y_i(t) \right), \end{cases} \quad i \bmod(6). \quad (4)$$

The characteristic equation for the trivial equilibrium is

$$Q(\lambda, \tau) = \left(\beta + (k - \varepsilon\alpha)\lambda + \lambda^2 \right)^6 - \left(k\lambda e^{-\lambda\tau} \right)^6 = 0. \quad (5)$$

In the absence of coupling delay ($\tau = 0$), the characteristic equation of Eq. (5) has the roots $\lambda_{1,2} = \left(\varepsilon\alpha \pm \sqrt{\varepsilon^2\alpha^2 - 4\beta} \right) / 2$. It implies that the trivial equilibrium is unstable because of $\mathrm{Re}(\lambda_{1,2}) > 0$ for the system parameters $\alpha > 0$ and $\varepsilon > 0$. In order to obtain the rhythm activity in the VDP-CPG controller, we determine the critical value of coupling delay for the Hopf bifurcation. Substituting $\lambda = i\omega, (\omega > 0)$ into $Q(\lambda, \tau) = 0$ gives

$$Q(i\omega, \tau) = \left(\beta + (k - \varepsilon\alpha)i\omega - \omega^2 \right)^6 + k^6\omega^6 \cos(6\omega\tau) - i k^6\omega^6 \sin(6\omega\tau) = 0. \quad (6)$$

Separating the real and imaginary parts of Eq. (6) yields

$$\begin{cases} k^6\omega^6 \cos(6\omega\tau) + q_1(\omega) = 0, \\ k^6\omega^6 \sin(6\omega\tau) - q_2(\omega) = 0, \end{cases} \quad (7)$$

where

$$\begin{aligned} q_1(\omega) &= \left(\beta + (k - \varepsilon\alpha - \omega)\omega \right) \cdot \left(\beta - \omega(k - \varepsilon\alpha + \omega) \right) \cdot \\ &\quad \left(\beta^2 + 2\beta(2k - 2\varepsilon\alpha - \omega)\omega + \omega^2((k - \varepsilon\alpha)^2 - 4(k - \varepsilon\alpha)\omega + \omega^2) \right) \cdot \\ &\quad \left(\beta^2 - 2\beta\omega(2k - 2\varepsilon\alpha + \omega) + \omega^2((k - \varepsilon\alpha)^2 + 4(k - \varepsilon\alpha)\omega + \omega^2) \right), \\ q_2(\omega) &= \omega \left(2(k - \varepsilon\alpha)(\beta - \omega^2)(-\beta^2 + (2\beta + 3(k - \varepsilon\alpha)^2)\omega^2 - \omega^4) \right) \cdot \\ &\quad \left(-3\beta^2 + (6\beta + (k - \varepsilon\alpha)^2)\omega^2 - 3\omega^4 \right). \end{aligned}$$

Solving τ from Eq. (7) and applying $\cos^2 6\omega\tau + \sin^2 6\omega\tau = 1$, one has

$$q_1^2(\omega) + q_2^2(\omega) - k^{12}\omega^{12} = 0, \tag{8}$$

In general, Eq. (8) is a 24-order polynomial equation and proposes at most 12 positive and simple roots. To simplify, we assume Eq. (8) just has two positive roots $\omega_1 > \omega_2 > 0$. It follows from Eq. (7) that time delay has the critical values

$$\tau_i^j = \frac{\varphi_i + 2j\pi}{6\omega_i}, \qquad i = 1, 2; j = 0, 1, 2, \cdots, \tag{9}$$

where $\varphi_i \in [0, 2\pi)$ and satisfied with $\cos\varphi_i = -q_1(\omega_i)/k^6\omega_i^6, \sin\varphi_i = q_2(\omega_i)/k^6\omega_i^6$. To present the transversality condition of the Hopf bifurcation, we differentiate $Q(\lambda, \tau) = 0$ with respect to τ and obtain

$$\frac{d\lambda}{d\tau} = \frac{k^6\lambda^7}{k^6\lambda^5(1 - \lambda\tau) - e^{6\lambda\tau}(k - \varepsilon\alpha + 2\lambda)(\beta + \lambda(k - \varepsilon\alpha + \lambda))^5}. \tag{10}$$

By the Hopf bifurcation theory, we obtain that the trivial equilibrium changes its stability by undergoing the Hopf bifurcations at the critical values of time delay with the transversality condition $\mathrm{Re}(d\lambda/d\tau) \neq 0$.

We choose the system parameters $\alpha = 1, \beta = 1, \varepsilon = 0.03, k = 0.8$ to analyze the Hopf bifurcation. It follows from Eq. (8) that the frequencies of the periodic activity are $\omega_1 = 1.11438$ and $\omega_2 = 0.89736$. The critical delays of the Hopf bifurcation are

$$\tau_1^0 = 0.3061, \tau_1^1 = 1.4731, \tau_1^2 = 2.6401, \tau_1^3 = 3.8071, \tau_1^4 = 4.9741, \tau_1^5 = 6.1410, \cdots, \tag{11}$$

and

$$\tau_2^0 = 0.6932, \tau_2^1 = 1.6329, \tau_2^2 = 2.5726, \tau_2^3 = 3.5123, \tau_2^4 = 4.4520, \tau_2^5 = 5.3917, \cdots. \tag{12}$$

Time histories and corresponding eigenvalues are illustrated in Fig. 3 for the fixed time delay that is in the parameter regions determined by the above critical values of (11) and (12). It follows that system (3) proposes a periodic activity when time delay subjects $\tau < \tau_1^0$, as shown in Fig. 3(a1) for time history with $\tau = 0.1$. The maximum eigenvalues are a conjugate pair with the positive real part, as shown in Fig. 3(a2). The dynamic behavior near the trivial equilibrium is a stable periodic activity. With increasing of time delay, the conjugate pair of the eigenvalues comes back to the left-right complex plane, as shown in Fig. 3(b2) for $\tau = 0.5$. It implies that the periodic activity evolves into a stable equilibrium, as shown in Fig. 3(b1). Further, the stable equilibrium will lose its stability and enter a periodic activity by employing the Hopf bifurcation when time delay is fixed as $\tau = 1$, which belongs to the intervals determined by τ_2^0 and τ_1^1, as shown in Fig. 3(c1). The conjugate pair of eigenvalues has the maximum real positive parts, as shown in Fig. 3(c2). Increasing time delay and going through the critical delay τ_1^1, the periodic activity evolves into the stable trivial

8

equilibrium, as shown in Fig. 3(d1) for $\tau = 1.6$. At this time, the maximum eigenvalues are a conjugate pair with the negative real part, as shown in Fig. 3(d2). It follows from Figs. 3(e1) and (e2) that system (3) will prepsent a stable periodic activity when time dealy increases and passes through the critical vlaues τ_2^1. In a word, employing the forward and backward Hopf bifurcation of the trivial equilibrium, the delayed VDP-CPG controller presents multiple stability switching from the periodic activity to equilibrium, and at last back to the periodic activity as time delay increases and passes through the above-mentioned critical delay values. Employing the procedure of the stability switching, the periodic activity will propose different spatiotemporal patterns, which can be used to construct the gait of the hexapod locomotion.
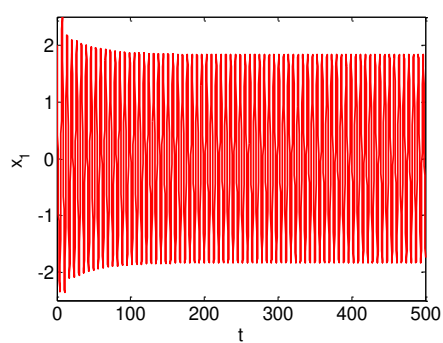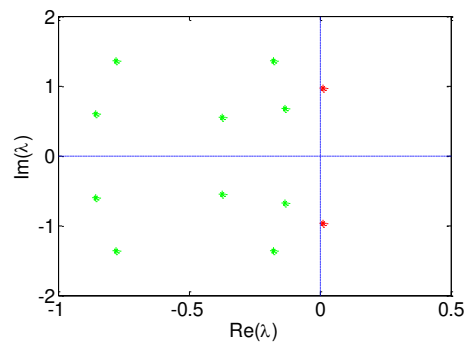
(a1)   (a2)
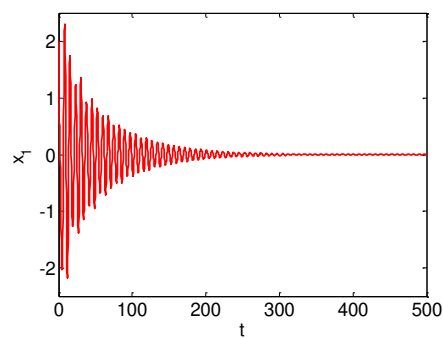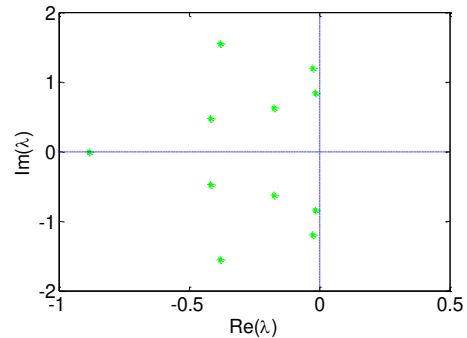
(b1)   (b2)
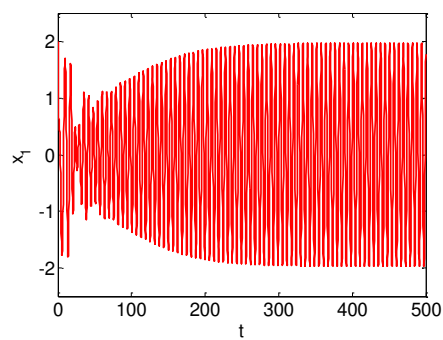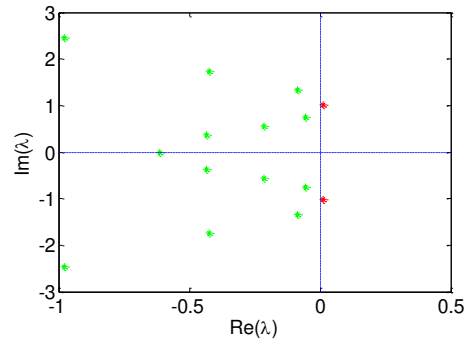
(c1)   (c2)
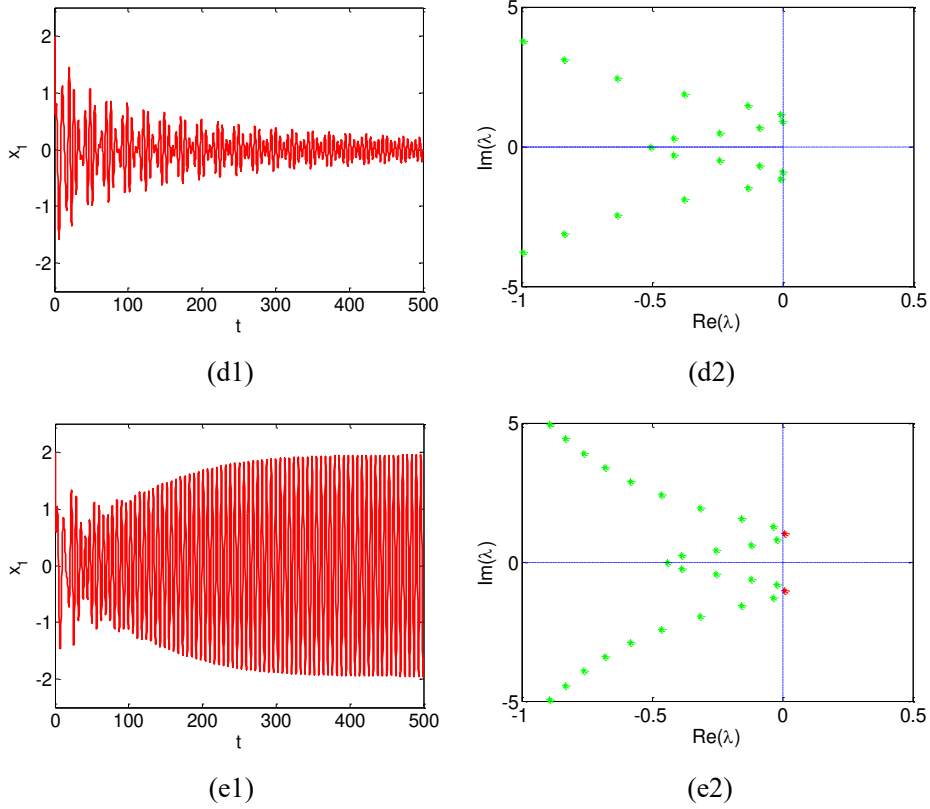
Fig. 3. Time histories (left) and corresponding eigenvalues (right) illustrate periodic activities to appear and disappear with increasing time delay (a) $\tau = 0.1$, (b) $\tau = 0.5$, (c) $\tau = 1$, (d) $\tau = 1.6$, and (e) $\tau = 2$ for the fixed parameters $\alpha = 1$, $\beta = 1$, $\varepsilon = 0.03$, and $k = 0.8$ in system (3).

4. Spatiotemporal patterns of bifurcating periodic activities

In the previous section, we have proposed the stable periodic activity for the delayed VDP-CPG controller by employing the Hopf bifurcation with increasing of time delay. To realize gait locomotion of the hexapod, the periodic activities produced by the VDP oscillators should propose multiple types of phase difference to present special patterns. In the following, we will analyze how symmetry of the VDP-CPG controller help to generate multiple spatiotemporal patterns and achieve gait switching of the hexapod locomotion.

To this end, the above-mentioned delayed VDP-CPG controller should be reformulated into a functional differential equation in the Banach space of continuous mapping from $[-\tau, 0]$ to R^{12}, i.e. $C = C([-\tau, 0], R^{12})$ and study its symmetry of the periodic solution generated by the Hopf bifurcation. Let $u_t = \left(x_1(t), y_1(t), x_2(t), y_2(t), \cdots, x_6(t), y_6(t) \right)^T \in C$ and define $u_t(\psi) = u(t + \psi)$, for $\psi \in [-\tau, 0]$. System (3) can be rewritten as

$$u_t' = h(u_t), \tag{13}$$

where

$$h_i(\phi) = \begin{pmatrix} \phi_{2i}(0) \\ -\beta\phi_{2i-1}(0) + (\alpha\varepsilon + k)\phi_{2i}(0) + k\phi_{2(i+5)}(\tau) - \varepsilon\phi_{2i-1}^2(0) \end{pmatrix}, \quad i\bmod(6). \quad (14)$$

Separating the linear parts from system (13) yields

$$u_t' = L(\tau)u_t, \quad (15)$$

where the linear operator $L(\tau): C \to R^{12}$ is defined by

$$L(\tau)\phi = \begin{pmatrix} \phi_{2i}(0) \\ -\beta\phi_{2i-1}(0) + (\alpha\varepsilon + k)\phi_{2i}(0) + k\phi_{2(i+5)}(\tau) \end{pmatrix}, \quad i\bmod(6). \quad (16)$$

It follows that the linear system (15) produces a strongly continuous semi-group of linear operators with infinitesimal generator $A(\tau)$ given as

$$A(\tau)\phi = \dot{\phi}, \quad \phi \in \mathrm{Dom}(A)$$
$$\mathrm{Dom}(A(\tau)) = \{\phi \in C : \dot{\phi} \in C, \dot{\phi}(0) = L(\tau)\phi\}. \quad (17)$$

Moreover, the eigenvalues of $A(\tau)$ correspond to the roots of the characteristic equation (5). Let Γ be a compact group. It follows that $u_t' = h(u_t)$ is Γ-equivariant if $h(\gamma u_t) = \gamma h(u_t)$ for all $\gamma \in \Gamma$. We focus on the case in the delayed VDP-CPG controller, i.e. $\Gamma = Z_6$, the cyclic group of order 6, with generator γ, where the action of Z_6 on R^{12} is given by

$$\gamma(u_i) = u_{i+6}, \quad \text{for all } i\bmod(12) \text{ and } u \in R^{12}. \quad (18)$$

It follows from the previous section that the characteristic equation has a pair of pure imaginary roots $\pm i\omega_{1,2}$ at the critical values $\tau_{1,2}^j$. The corresponding eigenvectors can be chosen as

$$\begin{cases} \xi_0 = (\eta_{1,2}, \eta_{1,2}, \eta_{1,2}, \eta_{1,2}, \eta_{1,2}, \eta_{1,2}), \\ \xi_1 = (\eta_{1,2}, \chi_1\eta_{1,2}, \chi_1^2\eta_{1,2}, \chi_1^3\eta_{1,2}, \chi_1^4\eta_{1,2}, \chi_1^5\eta_{1,2}), \ \chi_1 = \exp(\pi i/6), \\ \xi_2 = (\eta_{1,2}, \chi_2\eta_{1,2}, \chi_2^2\eta_{1,2}, \chi_2^3\eta_{1,2}, \chi_2^4\eta_{1,2}, \chi_2^5\eta_{1,2}), \ \chi_2 = \exp(2\pi i/6), \\ \xi_3 = (\eta_{1,2}, \chi_3\eta_{1,2}, \chi_3^2\eta_{1,2}, \chi_3^3\eta_{1,2}, \chi_3^4\eta_{1,2}, \chi_3^5\eta_{1,2}), \ \chi_3 = \exp(3\pi i/6), \\ \xi_4 = (\eta_{1,2}, \chi_4\eta_{1,2}, \chi_4^2\eta_{1,2}, \chi_4^3\eta_{1,2}, \chi_4^4\eta_{1,2}, \chi_4^5\eta_{1,2}), \ \chi_4 = \exp(4\pi i/6), \\ \xi_5 = (\eta_{1,2}, \chi_5\eta_{1,2}, \chi_5^2\eta_{1,2}, \chi_5^3\eta_{1,2}, \chi_5^4\eta_{1,2}, \chi_5^5\eta_{1,2}), \ \chi_5 = \exp(5\pi i/6), \end{cases} \quad (19)$$

where $\eta_1 = (1, i\omega_1)$ for τ_1^j, $\eta_2 = (1, i\omega_2)$ for τ_2^j, $j = 0, 1, \cdots, n$. The corresponding generalized eigenspace, $U_{i\omega_{1,2}}$, is spanned by the eigenfunctions $\mathrm{Re}(e^{i\omega_{1,2}\theta}\xi_k)$, $\mathrm{Im}(e^{i\omega_{1,2}\theta}\xi_k)$, that is

$$U_{i\omega_{1,2}} = \{x_1 e_1(\theta) + x_2 e_2(\theta), x_1, x_2 \in R\}, \quad (20)$$

where

$$e_1(\theta) = \cos(\omega_{1,2}\theta)\operatorname{Re}(\xi_k) - \sin(\omega_{1,2}\theta)\operatorname{Im}(\xi_k),$$
$$e_2(\theta) = \sin(\omega_{1,2}\theta)\operatorname{Re}(\xi_k) - \cos(\omega_{1,2}\theta)\operatorname{Im}(\xi_k).$$

Let $\omega = 2\pi/\omega_{1,2}$ and denoted by SP_ω the set of all ω-periodic solutions of system. Then

$$SP_\omega = \{x_1 e_1(t) + x_2 e_2(t), x_1, x_2 \in R\}. \tag{21}$$

Applying $Z_6 \times S^1$ on SP_ω results in

$$(\gamma, e^{i\theta})x(t) = \gamma x(t+\theta),$$
$$(\gamma, \theta) \in Z_6 \times S^1, x \in SP_\omega. \tag{22}$$

Let $\Sigma^\theta = \{(\gamma, e^{2\pi\theta i/\omega}), \theta \in (0, \omega)\}$, and let $\operatorname{Fix}(\Sigma^\theta, SP_\omega)$ be the fixed point set of Σ^θ under the action $Z_6 \times S^1$,

$$\operatorname{Fix}(\Sigma^\theta, SP_\omega) = \{x(t) \in SP_\omega; (\gamma, e^{i\theta})x = x \text{ for all } (\gamma, e^{i\theta}) \in \Sigma^\theta\}. \tag{23}$$

With similar notations of Wang and Campbell (2017), we obtain the following conclusions by applying the equivariant Hopf bifurcation of the delay differential equation. When the characteristic equation has a pair of pure imaginary roots $\pm i\omega_{1,2}$ at the critical values $\tau_{1,2}^j$ under the transversality conditions, the spatiotemporal symmetry of the Hopf bifurcating periodic solutions in system (5) can be completely characterized by $\operatorname{Fix}(\Sigma^\theta, SP_\omega)$. For the critical delayed values $\tau_{1,2}^j$, there exists a bifurcation of periodic solutions in system (5) with period T near $\omega = 2\pi/\omega_{1,2}$ and satisfying

$$u_{i-pm}(t) = u_i\left(t - p\frac{kT}{6}\right), \tag{24}$$
$$i = 1, 2, \ p = 1, \cdots, 5, k = 1, \cdots, 5. \ i, i-pm, pk(\operatorname{mod}12).$$

In fact, the periodic activities bifurcating from the corresponding critical values propose different phase difference. Specifically, the fully-synchronous patterns from the first critical value of time delay have the forms $(x(t), x(t), x(t), x(t), x(t), x(t))$, which is referred as in-phase locked oscillation (IPLO). An example case is shown in Fig. 4(a) for the fixed time delay $\tau = 0.1$, where the system parameters are fixed as $\alpha = 1, \beta = 1, \varepsilon = 0.03$, and $k = 0.8$ mentioned in the above section. With increasing time delay to $\tau = 1$, the IPLO shifts its phase difference and evolves into an out-of-phase synchronous periodic activity with $T/6$-phase difference, where T is a period time. The solution pattern proposes the form $(x(t), x(t+T/6), x(t+2T/6), x(t+3T/6), x(t+4T/6),$ $x(t+5T/6))$, called as the $T/6$-phase head-locked oscillation ($T/6$-PHLO). The time history is presented in Fig. 4(b). Further, when time delay is fixed as $\tau = 2$, the periodic activity presents a

new form with $T/3$-phase difference, called as $T/3$-phase head-locked oscillation ($T/3$-PHLO). The solution pattern is $\left(x(t), x(t+T/3), x(t+2T/3), \; x(t), x(t+T/3), x(t+2T/3)\right)$, as shown in Fig. 4(c). The anti-phase locked oscillations (APLO) $\left(x(t), x(t+T/2), x(t), x(t+T/2),\right.$ $\left. x(t), x(t+T/2)\right)$ are presented in Fig. 4(d) for the fixed time delay $\tau = 3$. Moreover, the periodic activity of the delayed VDP-CPG controller proposes $2T/3$- and $5T/6$-phase differences for the corresponding delayed regions, which is $T/3$ and $T/6$ lagging phase difference. We called these activities as the $T/3$-phase lag-locked oscillation ($T/3$-PLLO) and $T/6$-PLLO, respectively. The periodic activities have the corresponding solution forms $\left(x(t), x(t-T/3), x(t-2T/3), x(t),\right.$ $\left. x(t-T/3), x(t-2T/3)\right)$ and $\left(x(t), x(t-T/6), x(t-2T/6), x(t-3T/6), x(t-4T/6),\right.$ $\left. x(t-5T/6)\right)$, as presented in Figs. 4(e) and (f) with $\tau = 4$ and $\tau = 5.2$, respectively. Following this way, the periodic activities change their spatiotemporal patterns from IPLO to multiple types of out-of-phase synchronous oscillations with increasing time delay.

(a)   (b)

(c)   (d)
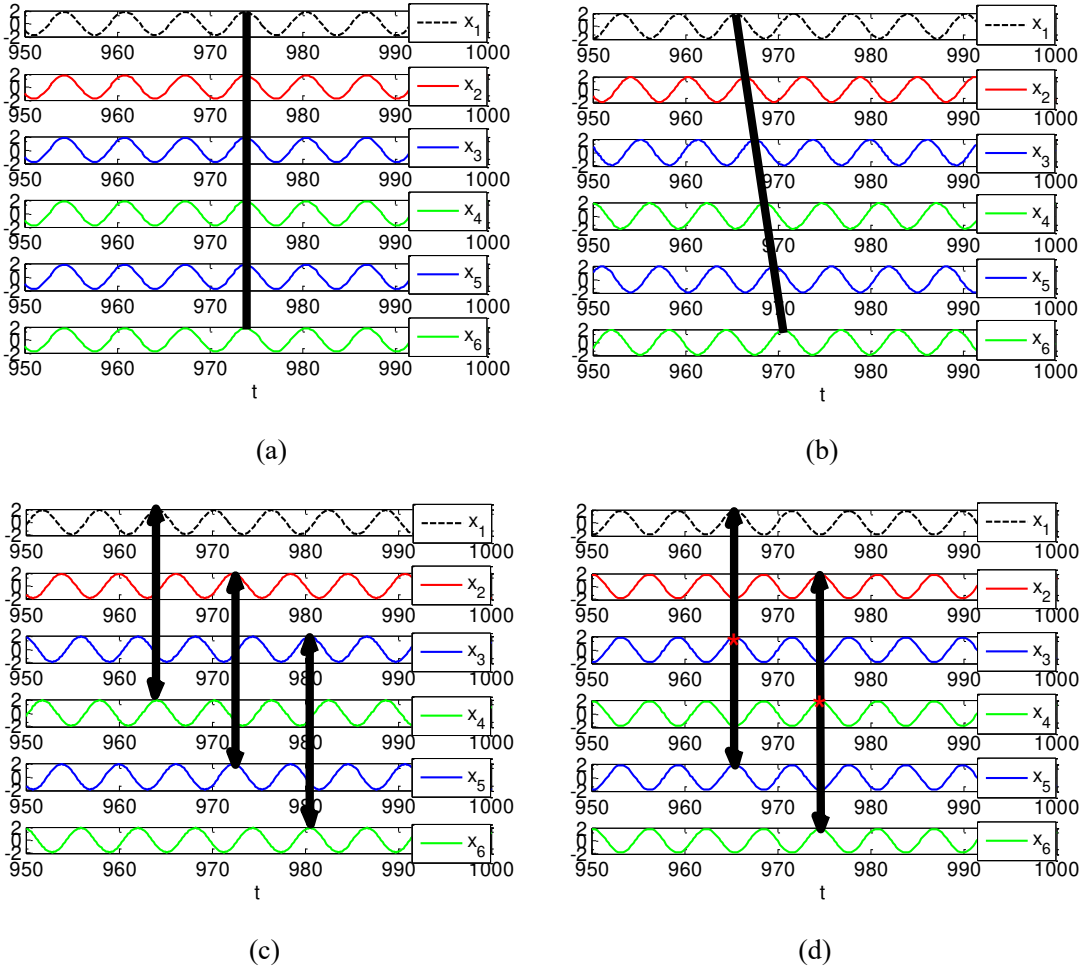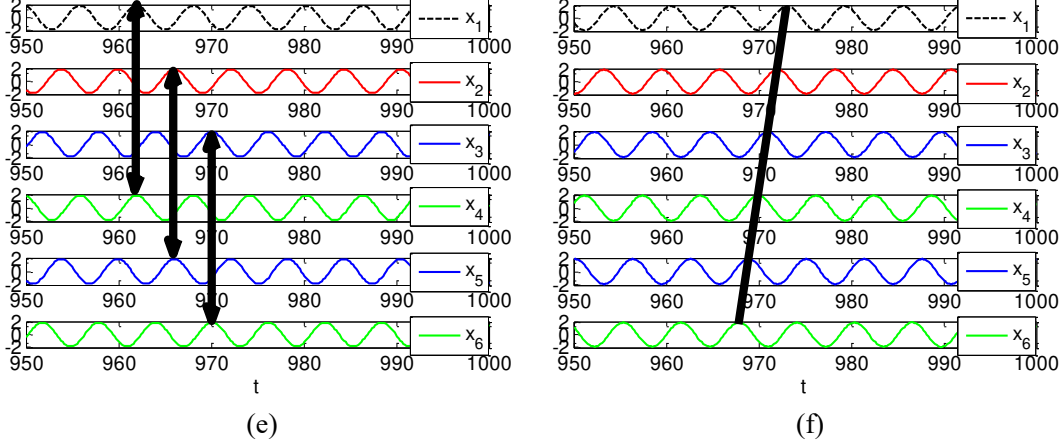
Fig. 4. Time histories illustrate the spatiotemporal patterns of the delayed VDP-CPG controller with increasing time delay (a) IPLO for $\tau = 0.1$, (b) $T/6$-PHLO for $\tau = 1$, (c) $T/3$-PHLO for $\tau = 2$, (d) APLO for $\tau = 3$, (e) $T/3$-PLLO for $\tau = 4$, and (f) $T/6$-PLLO for $\tau = 5.2$, where $\alpha = 1$, $\beta = 1$, $\varepsilon = 0.03$, and $k = 0.8$.

Based on the above-mentioned analysis, we illustrate the Hopf bifurcation curves to obtain the parameter regions with different spatiotemporal patterns, as shown in Fig. 5 for $\alpha = 1$, $\beta = 1$, and $\varepsilon = 0.03$. The (k, τ)-plane of the system parameters is classified into different regions, where the periodic activity bifurcating from the trivial equilibrium presents different phase difference, such as T/6, $T/3$, and $T/2$ due to Z_6 symmetry. It follows from Fig. 5 that Region I (referred as IPLO) is to the fully-synchronous periodic activity, which can be used to construct pronk gait of the hexapod locomotion. In region II ($T/6$-PHLO) and VI ($T/6$-PLLO), the periodic activities present $T/6$-phase difference (leading difference for II and lagging for VI) and can be used to construct wave, metachronal, and rolling tripod for different coupling sequence. Further, the locomotion gaits involved $T/3$, i.e. caterpillar and rice are obtained by choosing the system parameters in Region III ($T/3$-PHLO) and V ($T/3$-PLLO) for appropriate connection sequences. At last, tripod and pace gaits are to the Region IV (APLO), where the periodic activities propose $T/2$-phase difference.
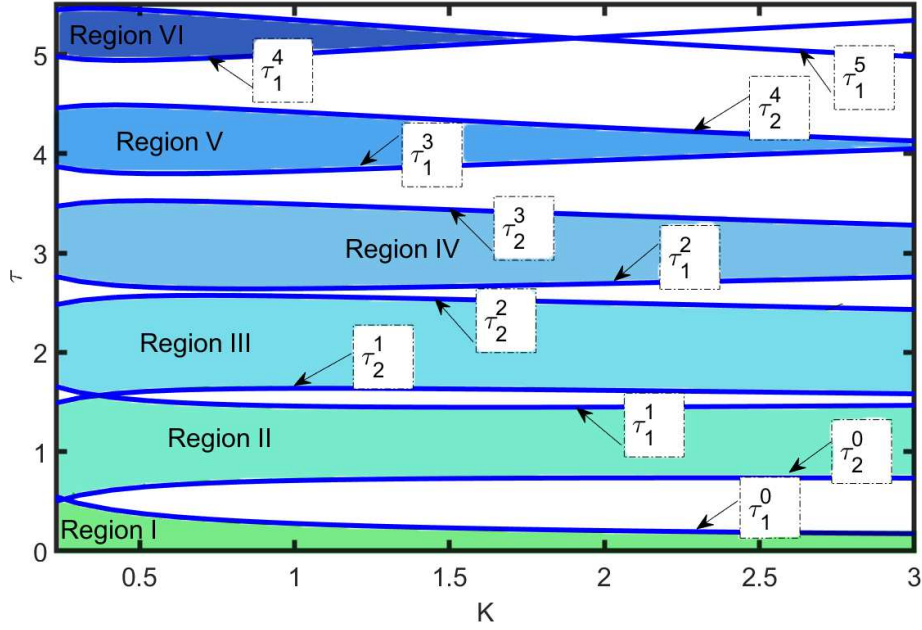
Fig. 5. The classification regions of periodic activities with different spatiotemporal patterns by employing the Hopf bifurcation curves, where $\alpha = 1$, $\beta = 1$, and $\varepsilon = 0.03$.

We further exhibit the phase difference of the periodic activities to present the robustness of the signal outputs constructed by the delayed VDP-CPG controller. It follows that the classification regions proposing the periodic activities with different spatiotemporal patterns is determined by the phase differences. The normalized phase differences of the periodic activities are given as

$$\Delta\phi_{1m} = \frac{t_1^{n+1} - t_m^n}{t_m^{n+1} - t_m^n}, \quad m = 2, \cdots, 6, \tag{25}$$

where the output signal of the first oscillator x_1 is as the reference, $t_m^n, m = 2, \cdots 6$ denote the time at which the m-th oscillator passes through the threshold for the n-th time. It follows from Eq. (25) that the phase difference of the periodic activity will be between 0 and 1. The fully-synchronous periodic activity corresponds to a zero-phase difference. The normalized 1/2-phase difference is to an anti-phase locked periodic activity. Further, 1/6 and 1/3 are to the other out-of-phase patterns of the periodic activity, as shown in Fig. 6. The numerical simulations validate theoretical results obtained by the equivariant Hopf bifurcation theory of the delay differential equation. It follows that these typical periodic activity having different spatiotemporal patterns will remain their phase difference as coupling weight k increases, which provides the robustness of signal outputs to construct the CPG controller for a wider space region of the parameters.
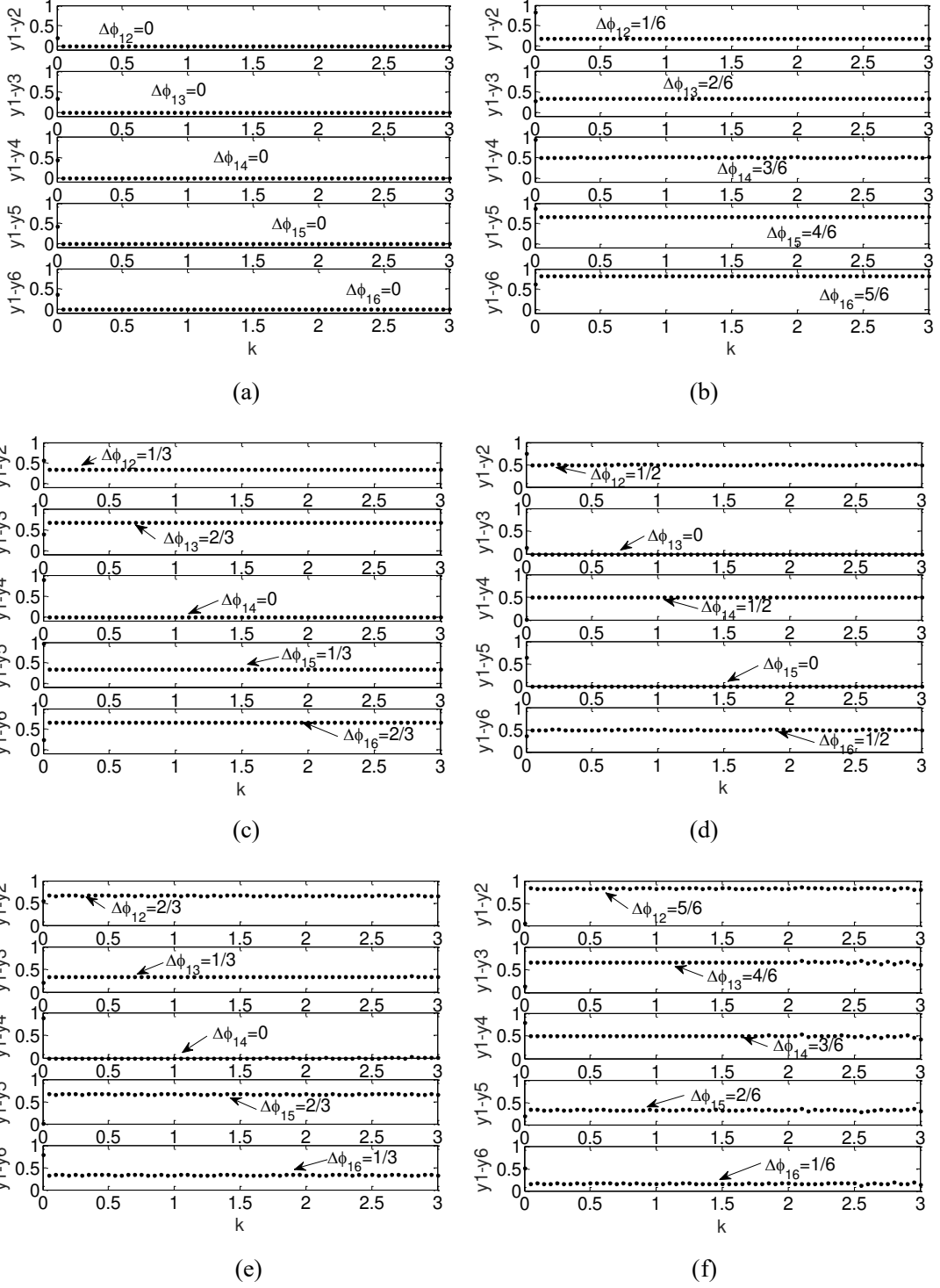
Fig. 6.   Phase differences with increasing coupling weight k illustrate the robustness of the gaits in the different parameter regions (a) $\tau = 0.1$, (b) $\tau = 1$, (c) $\tau = 2$, (d) $\tau = 3$, (e) $\tau = 4$, and (f) $\tau = 5.2$, where $\alpha = 1$, $\beta = 1$, $\varepsilon = 0.03$.

5. Gaits designing for hexapod locomotion

In the aforementioned studies, we have investigated the spatiotemporal patterns of the periodic activity by employing the equivariant Hopf bifurcation theory of the delay differential equation. The delayed VDP-CPG controller having the unidirectional ring structure displays different periodic activities due to Z_6 symmetry of the system. Further, by employing the Hopf bifurcation curves, we presented the corresponding parameter regions for the different spatiotemporal patterns. In the following section, we discuss how such the controller network is linked to the hexapod's legs to produce locomotion gaits. For a better understanding, we fix the connection between hexapod legs and the VDP oscillators. The legs of LF, LM, LH, RH, RM, and RF are controlled by the signal outputs of the i-th VDP oscillator, $i = 1, \cdots, 6$, as shown in Fig. 2(d). That is to say, oscillator 1 is to the LF leg and oscillator 2 is to LM leg, as so on. In order to produce the locomotion gaits of the hexapod robot, we construct phase difference of the six legs by switching connection order of the VDP oscillators. The legs' assignment is illustrated in Table 2. The first VDP oscillator controlling the LF leg is regarded as the reference unit. Notably, all constructed networks have a uniform topological structure, i.e. the unidirectional ring with identical oscillators. Further, we just present one of topological networks as an example for each case in Table 2. In fact, one gait maybe correspond to several assignment orders. An example is given in Fig. 7 to illustrate eight types of connection orders of the oscillators for tripod gait. All connections having unidirectional ring topology present tripod gait of the hexapod robot as the system parameters are fixed in Region IV, where signal outputs of the VDP oscillators illustrate the anti-phase locked oscillations.
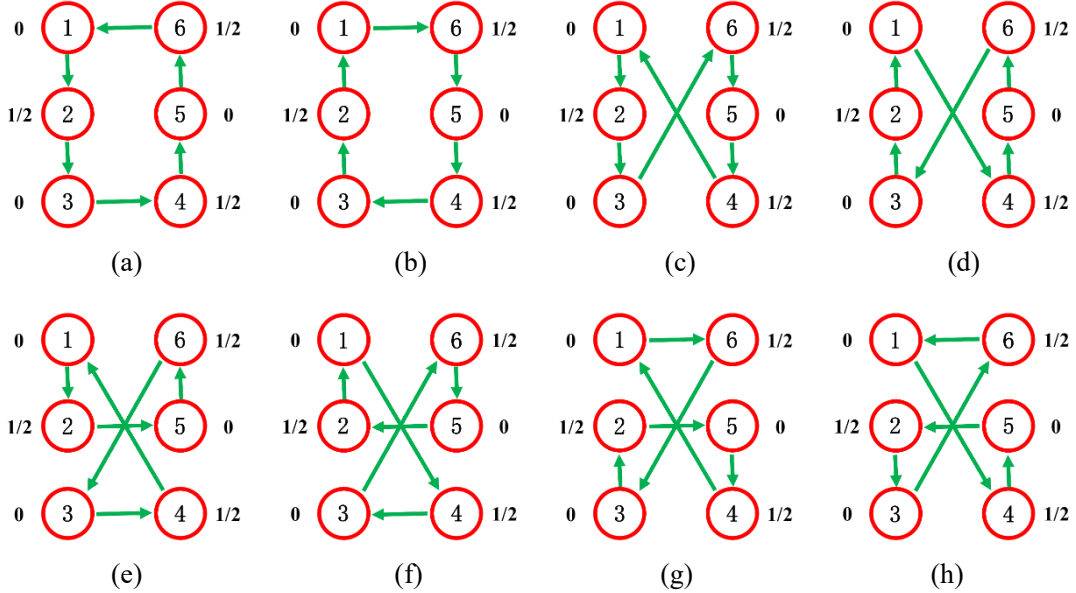

Fig. 7. Eight types of connection orders having unidirectional ring topology can present tripod gait of the hexapod robot as the system parameters are fixed in Region IV, where the signal outputs of the VDP oscillators illustrate the anti-phase locked oscillations.

Table 2: Spatiotemporal patterns are designed to present locomotion gaits of hexapod robot by choosing connection order of the delayed VDP-CPG controller with the unidirectional ring topology

Critical Eigen	Oscillating Form	Parameter Region	Topological Network	Gait
ξ_0	$\big(x(t), x(t), x(t), x(t), x(t), x(t)\big)$	Region I	Any connection order	Pronk
ξ_1	$\big(x(t), x(t+T/6), x(t+2T/6),$ $x(t+3T/6), x(t+4T/6), x(t+5T/6)\big)$	Region II	①→④→②→⑤→③→⑥→①	Wave
			①→⑥→⑤→④→③→②→①	Metachronal
			①→⑥→②→④→③→⑤→①	Rolling tripod
ξ_2	$\big(x(t), x(t+T/3), x(t+2T/3),$ $x(t), x(t+T/3), x(t+2T/3)\big)$	Region III	①→⑥→⑤→④→③→②→①	Caterpillar
			①→⑥→②→④→③→⑤→①	Rice
ξ_3	$\big(x(t), x(t+T/2), x(t),$ $x(t+T/2), x(t), x(t+T/2)\big)$	Region IV	①→⑥→⑤→④→③→②→①	Tripod
			①→④→②→⑤→③→⑥→①	Pace
ξ_4	$\big(x(t), x(t-T/3), x(t-2T/3),$ $x(t), x(t-T/3), x(t-2T/3)\big)$	Region V	Reversed direction	Caterpillar
			Reversed direction	Rice
ξ_5	$\big(x(t), x(t-T/6), x(t-2T/6),$ $x(t-3T/6), x(t-4T/6), x(t-5T/6)\big)$	Region VI	Reversed direction	Wave
			Reversed direction	Metachronal
			Reversed direction	Rolling tripod

It follows from Table 2 that the pronk gait is to the fully-synchronous periodic activity with zero-phase difference when the system parameters are fixed in Region I. At this time, the VDP oscillators of the delayed CPG controller can be assigned with any connection order. In Region II, the periodic activity with T/6-phase difference can be used to design three types of locomotion gaits, i.e. wave, metachronal, and rolling tripod for the hexapod robot. Specifically, wave gait is to the order assignment ①→④→②→⑤→③→⑥→①, where a backward propagation wave moves from the back to the forward. At this time, the order of the leg's movement is on the left side first and then on the right side, i.e., LF→RF→LM→RM→LH→RH. The adjacent legs, i.e. LF and LM, LM and LH, have T/3-phase difference. The contralateral legs, LF and RF, LM and RM, LH and RH, have T/6-phase difference. Metachronal gait has the order of the leg's movement, i.e. RH→RM→RF→LH→LM→LF, with the coupling connection ①→⑥→⑤→④→③→②→① for the delayed VDP-CPG controller. Similarly, when the VDP oscillators are connected as the order ①→⑥→②→④→③→⑤→①, the hexapod robot presents the rolling tripod gait with the order of leg's movement: LF→RH→LM→RF→LH→RM.

In Region III, the periodic activities of the delayed VDP-CPG controller have T/3-phase difference. For this case, switching topological structure of the oscillators can construct two types of gait, i.e. caterpillar and rice gaits. Caterpillar gait was proposed first by Golubitsky et al. (1998), where the left and right legs present synchronous activity, namely, {LF, RF}→{LM, RM}→{RH, LH}. The front and hind legs on opposite sides, i.e. LF and RH, LH and RF, have T/3-phase difference. The corresponding connection order of the units can be assigned as ①→⑥→⑤→④→

③→②→①. Rice gait, proposed first by Kitsunai et al. (2020) has synchronous patterns between the front and hind legs on opposite sides, namely, {LF, RH}→{LH, RF}→{RM, LM}. At this time, the contralateral legs, LF and RF, LH and RH, have T/3-phase difference, while LM and RM are in synchrony. In fact, the name of the gait pattern is derived from the corresponding Chinese characters or Japanese kanji sign.

In region IV, the periodic activity having T/2-phase difference can be used to construct the tripod and pace gaits, which proposes cyclical alternation of two phases. Tripod is a common and simple gait in entomological observations with high locomotion speed. In tripod gait, the ipsilateral front and back legs (LF and LH, RF and RH) and the contralateral middle legs (LM and RM) present synchronous activity. The legs in each segment propose T/2-phase difference. The adjacent legs on the right and left sides are also T/2-phase difference. That is to say, there are three legs swing or stand, delineating two intertwined triangles, i.e. {LF, RM, LH}→{RF, LM, RH}. To obtain the tripod gait, we can assign the corresponding connection order as ①→⑥→⑤→④→③→②→①, which is the same structure of the metachronal and caterpillar gait. In fact, the delayed VDP-CPG controller that we built can propose multiple types of locomotion gait with increasing time delay for the fixed topological structure due to the symmetry-breaking bifurcations. Further, we present the pace gait with increasing time delay for the identical structure of the wave gait, namely ①→④→②→⑤→③→⑥→①. In pace gait, the ipsilateral legs, namely LF, LM, LH, and RF, RM, RH have the same periodic activities. The left and right legs in each segment propose half a period out-of-phase, i.e. {LF, LM, LH}→{RF, RM, RH}.

In Regions V and VI, the delayed VDP-CPG controller proposes the periodic activities having T/3- and T/6-phase lag-locked oscillations. To obtain the same gaits of the hexapod locomotion exhibited in Table 1, we can just switch the connection direction of the VDP oscillators in the CPG controller. Of course, the unswitching direction of the proposed CPG controller will induce the corresponding revered gaits. Specifically, the reversed wave gait can be obtained for the same VDP-CPG controller having the wave gait as the system parameters are fixed in Region VI. Other reversed gaits can be derived in analogy. In fact, Inagaki et al. (2006) proposed the reversed metachronal and reversed rolling tripod, which can be obtained by using our delayed VPD-CPG controller for the metachronal and rolling tripod, as illustrated in Table 2.

At last, there are two types of gaits with T/4-phase difference, i.e. tetrapod and bowtie gaits for the hexapod locomotion. Tetrapod is a common gait with medium speed. The front and hind legs in the contralateral body, namely LF and RH, LH and RF, have synchronous patterns, which move together with zero-phase difference. Two legs of each segment have T/2-phase difference. The locomotion has a consecutive order, i.e. {RH, LF}→RM→{RF, LH}→LM. To obtain tetrapod gait, we adjust coupling delay to zero in the link connections of ④→③ and ⑥→①. The topological structure is labeled as ①→⑤→④=③→②→⑥=①, where → and = are denoted as the delayed and non-delayed connections, respectively. The system parameters including coupling delay and coupling weight are fixed in Region II for the case of the wave gait. The signal outputs of the CPG

controller present the tetrapod gait for the coupling parameters $\tau = 2$, $k = 0.8$ with the VDP oscillators $\alpha = 1$, $\beta = 1$, $\varepsilon = 0.03$, as illustrated in Fig. 8(a). Similarly, the bowtie gait, proposed by Kitsunai et al. (2020) from visual appearance of the network structure, can be obtained by fixing time delay as zero in the link connections of ②→③ and ④→⑤. The structure topology of the delayed VDP-CPG controller is presented as ①→⑥→②=③→④=⑤→①. In this case, the legs of the LF, RF, LM, and RM have T/4-phase difference. The left and right legs in the hind segment is synchrony to the corresponding middle legs, namely, LF→RF→{LM, LH}→{RM, RH}. The corresponding gait pattern is shown in Fig. 8(b), where the other system parameters are chosen as the tetrapod gait.
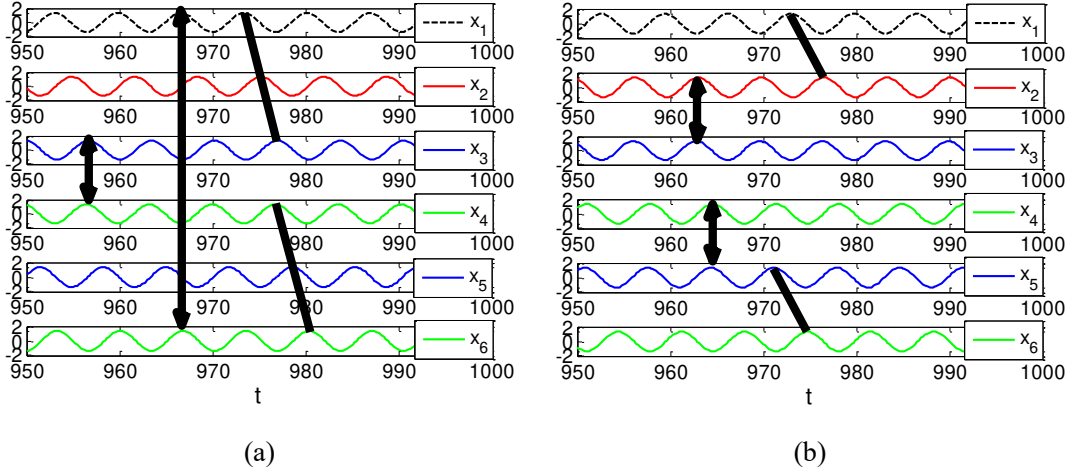

(a)　　　　　　　　　　　　　　(b)

Fig. 8.　(a) Tetrapod gait with the structure topology ①→⑤→④=③→②→⑥=① and (b) bowtie gait with ①→⑥→②=③→④=⑤→① for the delayed VDP-CPG controller for the system parameters $\alpha = 1$, $\beta = 1$, $\varepsilon = 0.03$, $k = 0.8$, $\tau = 2$, where → and = in the structure are denoted as the delayed and non-delayed connections, respectively.

6.　Conclusions

In this study, we constructed a new type of the delayed VDP-CPG controller and proposed an analysis method to obtain locomotion gaits of the hexapod robot. The topological structure of the CPG controller was designed as the unidirectional ring consisting of six identical VDP oscillator units. Employing the Hopf bifurcation of the delay differential equation, we presented the conditions of system parameters to guarantee the existence of period activity. The coupling delay between the VDP oscillators was regarded as the bifurcation parameter to steer the generation and extinction of the period activity. Due to the symmetry-breaking bifurcation, the periodic activity induced by the coupling delay proposes multiple types of phase difference. Based on the theoretical analysis of the equivariant Hopf bifurcation, we obtained the parameter regions divided by the Hopf bifurcation curves and explicated the relation of the corresponding parameter regions to the spatiotemporal patterns. Applying these period activities with constant phase difference, we assigned the coupling connection order of the VDP oscillators to produce multiple types of locomotion gaits of the hexapod robot. The results illustrated that the coupling delay in the delayed VDP-CPG controller is

an effective parameter to adjust many types of hexapodal locomotion gaits.

Acknowledgments

Statements and Declarations

Conflict of interest: The authors declare that they have no conflict of interest.

Data Availability Statement: Data sharing not applicable to this article as no datasets were generated or analysed during the current study.

References

Grillner, S., Manira, A.E.,: Current principles of motor control, with special reference to vertebrate locomotion. Physiol. Rev. 100(1), 271-320 (2020)

Wang, J., Chen, W., Xiao, X., Xu, Y., Li, C., Jia, X., Meng, M.Q.H.: A survey of the development of biomimetic intelligence and robotics. Bio. Intell. Robot. 1, 100001 (2021)

Lobato, R.V., Ramalingasetty, S.T., Özdil, P.G., Arreguit, J., Ijspeert, A.J., Ramdya, P.: NeuroMechFly, a neuromechanical model of adult drosophila melanogaster. Nat. Methods 19(5), 620-627 (2022)

Yu, J., Tan, M., Chen, J., Zhang, J.: A survey on CPG-inspired control models and system implementation. IEEE T. Neur. Net. Lear. 25(3), 441-456 (2014)

Kinugasa, T., Sugimoto, Y.: Dynamically and biologically inspired legged locomotion: A review. J. Robot. Mechatron. 29(3), 456-470 (2017)

Ryczko, D., Simon, A., Ijspeert, A.J.: Walking with salamanders: from molecules to biorobotics. Trends Neurosci. 43(11), 916-930 (2020)

Ijspeert, A.J., Crespi, A., Ryczko, D.: Cabelguen. From swimming to walking with a salamander robot driven by a spinal cord model. Science 315(5817), 1416–1420 (2007)

Ijspeert, A.J.: A connectionist central pattern generator for the aquatic and terrestrial gaits of a simulated salamander. Biol. Cybern. 84(5), 331–348 (2001)

Visarath, I., Andy, K., Patrick, L., Joseph, D.N., Antonio, P., Pietro, L.B.: Meet ANIBOT: The first biologically-inspired animal robot, Int. J. Bifurcat. Chaos 32(1), 2230001 (2022)

Shinkichi, I., Hideo, Y., Tamio, A.: CPG model for autonomous decentralized multi-legged robot system—generation and transition of oscillation patterns and dynamics of oscillators. Rob. Auton. Syst. 44, 171–179 (2003)

Inagaki, S., Yuasa, H., Suzuki, T.: Wave CPG model for autonomous decentralized multi-legged robot: Gait generation and walking speed control. Rob. Auton. Syst. 54(2), 118–126 (2006)

Goldman, D.I., Chen, T.S., Dudekand, D.M.: Dynamics of rapid vertical climbing in cockroaches reveals a template. J. Exp. Biol. 209(15), 2990–3000 (2006)

Holmes, P., Full, R.J., Koditschek, D.: The dynamics of legged locomotion: Models, analyses, and challenges. SIAM Rev. 48(2), 207–304 (2006)

Chen, W.H., Ren, G.J., Zhang, J.B., Wang, J.H.: Smooth transition between different gaits of a hexapod robot via a central pattern generators algorithm. J. Intell. Robot. Syst. 67, 255–270

(2012)

Jose, H.B.Z., Cesar, T.H., Bernard, G., Perception-driven adaptive CPG-based locomotion for hexapod robots. Neurocomputing 170, 63–78 (2015)

Yu, H., Gao, H., Ding, L., Li, M., Deng, Z., Liu, G.: Gait generation with smooth transition using CPG-based locomotion control for hexapod walking robot. IEEE T. Ind. Electron. 63, 5488-5500 (2016)

Wang, G., Chen, X., Han, S.K.: Central pattern generator and feedforward neural network-based self-adaptive gait control for a crab-like robot locomoting on complex terrain under two reflex mechanisms. Int. J. Adv. Robot Syst. 14(4), 1–13 (2017)

Chang, Q., Mei, F.H.: A bioinspired gait transition model for a hexapod robot. J. Robot. 2018, 2913636 (2018)

Cafer, B.: Neural coupled central pattern generator based smooth gait transition of a biomimetic hexapod robot. Neurocomputing 420, 210–226 (2021)

Ashwin, S.L., Yan, F., Justin, T., Arijit, R.: Learning to walk: bio-mimetic hexapod locomotion via reinforcement-based spiking central pattern generation. IEEE J. Em. Sel. Top. C. 10(4), (2020)

Ouyang, W., Chi, H., Pang, J., Liang, W., Ren, Q.: Adaptive locomotion control of a hexapod robot via bio-inspired learning. Front. Neurorobot. 15, 627157 (2021)

Martin, G., Ian, S., Pietro, L.B., Collins, J.J.: A modular network for legged locomotion. Physica D 115, 56-72 (1998)

Golubitsky, M., Stewart, I., Buono, P.L., Collins, J.: Symmetry in locomotor central pattern generators and animal gaits. Nature 401(6754), 693-695 (1999)

Martin, G., Ian, S.: Rigid patterns of synchrony for equilibria and periodic cycles in network dynamics. Choas 26, 094803 (2016)

Carla, M.P., Martin, G.: Central pattern generators for bipedal locomotion. J. Math. Biol. (2006) 53:474–489

Ian, S.: Symmetry-breaking in a rate model for a biped locomotion central pattern generator. Symmetry. 6, 23-66(2014)

Pietro, L.B., Martin, G.: Models of central pattern generators for quadruped locomotion I. Primary gaits. J. Math. Biol. 42, 291–326 (2001)

Pietro, L.B.: Models of central pattern generators for quadruped locomotion II. Secondary gaits. J. Math. Biol. 42, 327–346 (2001)

Ian, S.: Spontaneous symmetry-breaking in a network model for quadruped locomotion. Int. J. Bifurcat. Chaos 27(14), 1730049 (2017)

Collins, J.J., Ian, S.: Hexapodal gaits and coupled nonlinear oscillator models. Biol. Cybern. 68, 287-298 (1993)

Ghigliazza, R.M., Holmes, P.: A minimal model of a central pattern generator and motoneurons for insect locomotion. SIAM J. Appl. Dyn. Syst. 3(4), 671–700 (2004)

Zahra, A., Vaibhav, S., Holmes, P.: Gait transitions in a phase oscillator model of an insect central pattern generator. SIAM J. Appl. Dyn. Syst. 17(1), 626-671 (2018)

Zahra, A., Holmes, P.: Heterogeneous inputs to central pattern generators can shape insect gaits. SIAM J. Appl. Dyn. Syst. 18(2), 1037-1059 (2019)

Barrio, R., Lozano, Á., Rodríguez, M., Serrano, S.: Numerical detection of patterns in CPGs: Gait patterns in insect movement. Commun. Nonlinear Sci. Numer. Simulat. 82, 105047 (2020)

Song, Z., Xu, J., Zhen, B.: Multitype activity coexistence in an inertial two-neuron system with

multiple delays. Int. J. Bifurcat. Chaos 25(13), 1530040 (2015)

Song, Z., Zhen, B., Hu, D.: Multiple bifurcations and coexistence in an inertial two-neuron system with multiple delays. Cogn. Neurodyn. 14, 359–374 (2020)

Yao, S., Ding, L., Song, Z., Xu, J.: Two bifurcation routes to multiple chaotic coexistence in an inertial two-neural system with time delay. Nonlinear Dyn. 95, 1549–1563 (2019)

Sue, A.C., Yuan, Y., Sharene, D.B.: Equivariant Hopf bifurcation in a ring of identical cells with delayed coupling. Nonlinearity 18, 2827–2846 (2005)

Fatihcan, M.A., Haibo, R.: Symmetry analysis of coupled scalar systems under time delay. Nonlinearity 28, 795–824 (2015)

Wang, Z., Sue, A.C.: Symmetry, Hopf bifurcation, and the emergence of cluster solutions in time delayed neural networks. Choas 27, 114316 (2017)

Ohgane, K., Ei, S.I., Mahara, H.: Neuron phase shift adaptive to time delay in locomotor control. Appl. Math. Model. 33(2), 797-811 (2009)

Verdaasdonk, B., Koopman, H.F., Helm, F.C., Resonance tuning in a neuro-musculo-skeletal model of the forearm. Biol. Cybern. 96(2), 165-180 (2007)

Lu, Q., Wang, X., Tian, J.: A new biological central pattern generator model and its relationship with the motor units. Cogn. Neurodyn. 16(1), 135-147 (2022)

Zhu, Y.G., Wu, Y.S., Liu, Q., Guo, T., Qin, R., Hui, J.Z.: A backward control based on σ-Hopf oscillator with decoupled parameters for smooth locomotion of bio-inspired legged robot. Rob. Auton. Syst. 106, 165-178 (2018)

Zhu, Y., Zhou, S., Gao, D., Liu, Q.: Synchronization of non-linear oscillators for neurobiologically inspired control on a bionic parallel waist of legged robot. Front. Neurorobot. 13, 59 (2019)

Shunki, K., Woorim. C., Chihiro. S., Supat, S., Qin, Z.X., Yasuharu, K., Mattia, F., Natsue, Y., Ludovico, M.: Generation of diverse insect-like gait patterns using networks of coupled Rössler systems. Chaos 30, 123132 (2020)

Song, Z.G., Xu, J.: Self-/mutual-symmetric rhythms and their coexistence in a delayed half-center oscillator of the CPG neural system. Nonlinear Dyn. 108, 2595–2609 (2022)

Song, Z.G, Huang, X., Xu, J.: Spatiotemporal pattern of periodic rhythms in delayed Van der Pol oscillators for the CPG-based locomotion of snake-like robot. Nonlinear Dyn. 110, 3377–3393 (2022)